

Local time effects in satellite estimates of electromagnetic induction transfer functions

Georgios Balasis,¹ Gary D. Egbert,² and Stefan Maus^{1,3,4}

Received 1 April 2004; revised 14 July 2004; accepted 2 August 2004; published 28 August 2004.

[1] The current satellite magnetic missions offer new opportunities to determine the electrical conductivity of the Earth. However, satellites are nearly stationary in local time and therefore sample the inducing and induced fields quite differently than geomagnetic observatories, which rotate with the Earth. We show that estimates of induction transfer functions obtained from CHAMP magnetic data under the traditional symmetric magnetospheric ring current source (Y_1^0) assumption depend systematically on local time, suggesting that source fields contain also a coherent non-axisymmetric component. An extended magnetospheric source model that incorporates a coherent non-axisymmetric quadrupole (Y_2^1), and allows for Earth rotation qualitatively explains the observations. *INDEX TERMS*: 0619 Electromagnetics: Electromagnetic theory; 1515 Geomagnetism and Paleomagnetism: Geomagnetic induction; 2778 Magnetospheric Physics: Ring current; 3210 Mathematical Geophysics: Modeling. **Citation**: Balasis, G., G. D. Egbert, and S. Maus (2004), Local time effects in satellite estimates of electromagnetic induction transfer functions, *Geophys. Res. Lett.*, 31, L16610, doi:10.1029/2004GL020147.

1. Introduction

[2] Electromagnetic induction studies with satellite magnetic data may ultimately provide important new constraints on the electrical conductivity of Earth's mantle. In contrast to the spatially sparse geomagnetic observatory data, which provide the basis for most of our present knowledge about deep Earth conductivity [e.g., *Banks*, 1969; *Olsen*, 1998; *Fujii and Schultz*, 2002], data from a satellite cover the Earth completely over the course of some months. However, at any fixed time, sampling by a polar orbiting satellite is restricted to a single meridian. Interpretation of the time varying external fields in terms of Earth conductivity thus requires simplifying assumptions about the longitudinal structure of external sources. Most studies to date [e.g., *Olsen*, 1999; *Constable and Constable*, 2004] have assumed that long period external magnetic variations are due to a symmetric magnetospheric ring current, and are hence describable on the Earth's surface by an external geomagnetic axial dipole Y_1^0 . This simple model would appear to be supported by the observation that on the Earth's surface geomagnetic

variations for periods beyond about 5 days are very well approximated (at least at mid-latitudes) by a Y_1^0 source [*Banks*, 1969; *Fujii and Schultz*, 2002]. However, this conclusion is based on geomagnetic observatory data, which are sampled in a reference frame that rotates with the Earth. Non-axisymmetric source structure of degree n will result in variations of frequency $f \approx n$ cycles per day (cpd) in this rotating frame, so any low frequency ($f \ll 1$ cpd) variations observed in the Earth's frame will inevitably be nearly zonal.

[3] In fact it is well known that magnetospheric current systems are not symmetric with regard to the Earth's rotation (or geomagnetic dipole) axis [e.g., *Campbell*, 1997; *Daglis and Kozyra*, 2002]. For example, recent quantitative models of magnetospheric fields [*Tsyganenko*, 2002] incorporate a partial ring current which is driven by azimuthal variations of plasma pressure, and closes via Birkeland currents through the auroral ionosphere. It would thus be somewhat surprising if the resulting magnetic variations seen by a near-Earth satellite were purely zonal at any period. Indeed, *Constable and Constable* [2004] found significant differences between amplitudes of long period variations inferred from dawn and dusk Magsat passes, clearly showing that there is significant non-axisymmetric structure in the source fields. In this paper we show that estimates of induction transfer functions (TFs) obtained from CHAMP scalar data under the Y_1^0 source assumption depend systematically on local time (LT), and are thus significantly biased by these non-axisymmetric currents. Extending the simplest Y_1^0 source model to include a quadrupole (Y_2^1) source term that is temporally varying, but spatially fixed in a magnetospheric frame, qualitatively explains the observed LT effects.

2. CHAMP Data Processing

[4] Under the usual assumptions that the external sources are uniform (corresponding to a Y_1^0 surface harmonic), and that the Earth conductivity varies only with radius, the scalar magnetic anomaly observed by the satellite at $\mathbf{r} = (r, \theta, \phi)$ can be expressed as

$$B(\mathbf{r}, t) = q_{10}(t)h_{10}^e(\mathbf{r}) + g_{10}(t)h_{10}^i(\mathbf{r}) \quad (1)$$

with $h_{10}^e(\mathbf{r}) = \mathbf{b}(\mathbf{r}) \cdot (-\cos\theta, \sin\theta, 0)$ and $h_{10}^i(\mathbf{r}) = \mathbf{b}(\mathbf{r}) \cdot (2\cos\theta, \sin\theta, 0) (a/r)^3$. Here $\mathbf{b}(\mathbf{r})$ is a unit vector in the direction of the main field, θ is magnetic colatitude, a is the Earth radius, superscripts e and i denote components of external and internal origin, with time variations denoted by $q_{10}(t)$ and $g_{10}(t)$ respectively, and the Schmidt-normalization for the spherical harmonic basis functions is chosen.

[5] In the frequency domain the internal and external components are related by $\tilde{g}_1(\omega) = Q_1(\omega)\tilde{q}_1(\omega)$, where $Q_1(\omega)$

¹GeoForschungsZentrum Potsdam, Potsdam, Germany.

²College of Oceanic and Atmospheric Sciences, Oregon State University, Corvallis, Oregon, USA.

³Now at CIRES, University of Colorado, Boulder, Colorado, USA.

⁴Also at National Geophysical Data Center, National Oceanographic and Atmospheric Administration, Boulder, Colorado, USA.

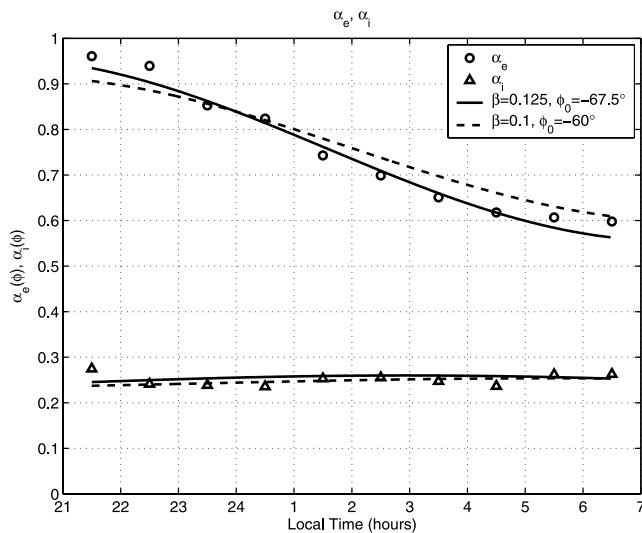


Figure 1. Proportionality constants $\alpha_e = q_{10}/D_{st}$ and $\alpha_i = g_{10}/D_{st}$ as a function of LT, estimated from CHAMP data (symbols), and computed for the quadrupole model with $\beta = 0.125$, and $\phi_0 = -67.5^\circ$ (solid lines), and with $\beta = 0.1$, and $\phi_0 = -60^\circ$ (dashed lines).

is the electromagnetic TF for a radially symmetric Earth excited by external sources of spherical harmonic degree 1 and angular frequency ω .

[6] To estimate Q_1 , time series of $q_{10}(t)$ and $g_{10}(t)$ were inferred from three years of CHAMP satellite magnetic field measurements. To avoid the known attitude uncertainties and limited coverage of the CHAMP vector data, total field measurements of the scalar magnetometer were used. For uninterrupted coverage we selected the 20–8 LT sector, which, from our experience, has the least contribution from ionospheric currents (for details on the estimation of $q_{10}(t)$ and $g_{10}(t)$ see *Maus and Weidelt* [2004]). The resulting time series, sampled at the CHAMP orbital frequency of 1.8×10^{-4} Hz, were analyzed with a scheme combining the robust SVD algorithm of *Egbert* [1997] with a wavelet analysis technique [*Balasis et al.*, 2004] to estimate $Q_1(\omega)$, which was then converted into the more standard C -response (on the definition of C -response see *Maus and Weidelt* [2004]).

[7] In addition to the full time series, we also analyzed subsets of data corresponding to different ranges of LTs. Because the CHAMP orbit plane precesses through all local times roughly once every four months, estimates of $q_{10}(t)$ and $g_{10}(t)$ corresponding to a four hour LT window (e.g., 20:00–24:00) are obtained in a series of distinct blocks of data, each about 1.3 months long. Wavelet analysis was done separately for each of these blocks, and wavelet coefficients for all blocks were then combined to yield estimates of the TF $Q_1(\omega)$ as a function of LT.

3. Results

[8] The estimates of $q_{10}(t)$ track the disturbed storm time index D_{st} fairly closely, with a squared correlation of $R^2 = 0.80$. Fitting the simple time domain regression models $q_{10}(t) = \alpha_e D_{st}(t)$, $g_{10}(t) = \alpha_i D_{st}(t)$ to the full three years of CHAMP dipole estimates, yields estimated proportionality constants $\hat{\alpha}_e = 0.69$ and $\hat{\alpha}_i = 0.23$. As D_{st} should be

comparable to $(q_{10} + g_{10})$ [*Langel and Hinze*, 1998], we expect $\alpha_e + \alpha_i = 1$. The discrepancy here ($\hat{\alpha}_e + \hat{\alpha}_i = 0.92$) probably reflects downward bias in the regression estimates due to “noise” in D_{st} [c.f. *Olsen*, 1998]. Adjusting the proportionality constants by dividing by 0.92 results in modified estimates $\hat{\alpha}_e = 0.75$ and $\hat{\alpha}_i = 0.25$. Fitting the same model to subsets of data sorted by LT reveals a clear systematic variation of α_e decreasing from 0.96 in early evening hours to 0.60 in the morning (Figure 1). There is no clear dependence of α_i on LT.

[9] D_{st} is computed from an average over 4 observatories around the equator, and hence serves as a proxy for a symmetric ring current. The observed LT dependence of α_e suggests that there are coherent non-axisymmetric components to ring current variations. These are averaged out in D_{st} , but systematically bias estimates of q_{10} obtained from fitting the simple model (1) to individual passes. Our results for night-side data are consistent with those obtained by *Schwarte* [2004] from a more extensive analysis of CHAMP vector data for all LTs.

[10] In Figure 2 estimated C_1 -responses are plotted for three non-overlapping four hour LT bands (20:00–24:00, 0:00–4:00, 4:00–8:00), and for all nightside data. Consistent with the results of Figure 1, there are clear and systematic variations of C_1 with LT. Not surprisingly, the response function estimated using all LTs is roughly an average of the 3 subset curves. This average curve also agrees well with the C_1 -response function for 0:00–4:00 LT (as might already be expected from the variations of α_e seen in Figure 1), and is in reasonable agreement with *Olsen’s* [1998] estimate of C_1 obtained from European observatory data (Figure 2). The estimated C -responses for the 4:00 to 8:00 LT sector have much higher uncertainty due to the weaker magnetospheric signal and possible contamination by modulations in ionospheric daily variation fields in the

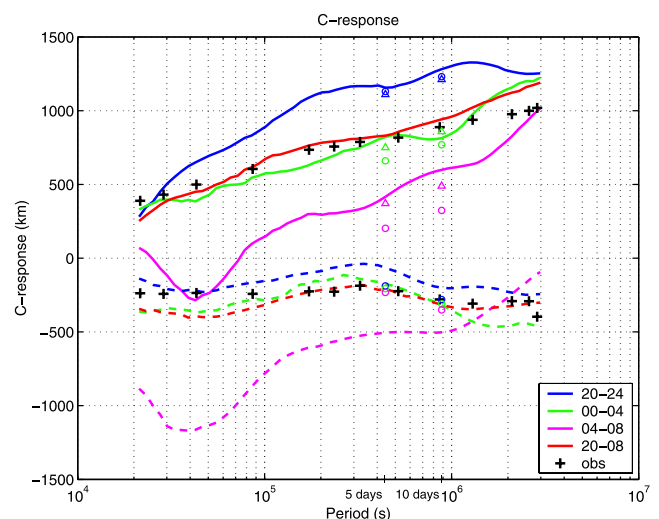


Figure 2. C_1 -response functions for 3 different LT subsets (20:00–24:00, 0:00–4:00 and 4:00–8:00) and for all nightside data. Solid and dashed lines denote real and imaginary parts, respectively, and crosses are observatory results from *Olsen* [1998]. LT variation of C_1 predicted by the quadrupole model are plotted for the same three local times at periods of $T = 5, 10$ days, for $\beta = 0.125$, and $\phi_0 = -67.5^\circ$ (circles), and $\beta = 0.1$, and $\phi_0 = -60^\circ$ (triangles).

morning sector. This was also reported by *Constable and Constable* [2004] for Magsat data.

4. Quadrupole Sources Over a Rotating Earth

[11] The dipole source model (1) corresponds to uniform external fields, as would result from a large symmetric ring current. The simplest extension which could explain the observed LT effects includes also a quadrupole source term with magnetic potential

$$V_{21}^e(\mathbf{r}, t) = (r^2/a)P_2^1(\cos\theta)\cos(\phi - \phi_0)q_{21}(t). \quad (2)$$

Here $P_2^1(\cos\theta)$ is the associated Legendre function of degree 2 and order 1 and ϕ is the magnetospheric longitude. Adding this term allows the magnetospheric variation fields to be stronger on one side of the Earth than the other, as would be expected if the ring current were asymmetric. In (2) we assume that ϕ_0 , which defines the longitudinal quadrupole orientation relative to local midnight, is constant. Our model is thus the simplest extension of the uniform source model allowing for large scale asymmetry in the ring current. The actual asymmetries in the magnetospheric sources are undoubtedly more complex [e.g., see *Tsyganenko*, 2002].

[12] The internal component induced by equation (2) requires some care, because the spatial structure of V_{21}^e is expressed in a reference frame fixed to the magnetosphere, while effects of induction must be computed in a frame rotating with the Earth. To keep derivations simple we ignore the distinction between geomagnetic and geographic coordinate systems, so that the transformation to Earth fixed coordinates takes the simple form $\phi - \phi_0 \rightarrow \phi' + \omega_r t$, where ω_r is the Earth's angular rotation rate and ϕ' is longitude on Earth.

[13] Consider long period variations of a fixed angular frequency $\omega \ll \omega_r$ with unit magnitude and zero phase. In the magnetospheric frame the external quadrupole potential can then be written $(r^2/2a)P_2^1(\cos\theta)\Re[e^{-i(\phi-\phi_0)}(e^{-i\omega t} + e^{i\omega t})]$. After transforming to the Earth frame, the external potential can be expressed as a sum of two quadrupole terms

$$(r^2/2a)P_2^1(\cos\theta)\Re\left[e^{-i\phi'}\left(e^{-i(\omega_r+\omega)t} + e^{-i(\omega_r-\omega)t}\right)\right] \quad (3)$$

of frequencies $\omega_r + \omega$ and $\omega_r - \omega$. For magnetospheric variations with periods exceeding a few days, $\omega \ll \omega_r$, and equation (3) can be approximated as $(r^2/a)P_2^1(\cos\theta)\Re[e^{-i\phi'}e^{-i\omega_r t}]$. Thus in an Earth fixed frame the inducing field is essentially of frequency ω_r , not ω . The internal component induced by equation (3) can be computed exactly in terms of the second degree TF $Q_2(\omega_r)$ evaluated at $\omega_r \pm \omega$. Making the approximation $Q_2(\omega_r \pm \omega) \approx Q_2(\omega_r)$ to compute the internal potential, and then transforming back to the magnetospheric frame we find

$$V_{21}^i(\mathbf{r}, t) = \frac{a^4}{r^3}P_2^1(\cos\theta)\Re\left[\underbrace{Q_2(\omega_r)}_{\kappa(\phi)}e^{-i(\phi-\phi_0)}\right]\cos(\omega t). \quad (4)$$

Note that $\kappa(\phi)$, which combines the 1 cpd induction TF with the longitudinal variation in the source, does not depend on ω . To the degree of approximation considered here there is no temporal phase shift between the internal and external

parts of the low frequency quadrupole variations. This makes sense, since the time lag associated with induction at a period of one day (on the order of an hour) corresponds to a very small phase shift for these longer periods. However, there is a shift in LT of the peak amplitudes of internal and external quadrupole terms, due to the relatively significant rotation of the Earth during the induced field time lag.

[14] Allowing for both dipole (q_{10}) and quadrupole (q_{21}) components of the long period variations we can thus approximate the scalar anomaly observed along a satellite track by

$$B(\mathbf{r}, t) = q_{10}(t)h_{10}^e(\mathbf{r}) + g_{10}(t)h_{10}^i(\mathbf{r}) + q_{21}(t)(h_{21}^e(\mathbf{r})\cos(\phi - \phi_0) + h_{21}^i(\mathbf{r})\kappa(\phi)) \quad (5)$$

where $h_{21}^e(\mathbf{r}) = \mathbf{b}(\mathbf{r}) \cdot \sqrt{3}(-\sin 2\theta, -\cos 2\theta, 0) (r/a)$ and $h_{21}^i(\mathbf{r}) = \mathbf{b}(\mathbf{r}) \cdot \sqrt{3}(\frac{3}{2}\sin 2\theta, -\cos 2\theta, 0) (a/r)^4$. For a single satellite track a straightforward calculation, assuming a dipolar main field, shows that if the model of equation (1) is fit with least squares — when equation (5) is in fact correct — estimates of the dipole terms take the form

$$\hat{q}_{10} = q_{10} + \underbrace{[H_{11}\cos(\phi - \phi_0) + H_{12}\kappa(\phi)]}_{c_1(\phi)}q_{21} \quad (6)$$

$$\hat{g}_{10} = g_{10} + \underbrace{[H_{21}\cos(\phi - \phi_0) + H_{22}\kappa(\phi)]}_{c_2(\phi)}q_{21} \quad (7)$$

where matrix $\mathbf{H} = \begin{pmatrix} \langle h_{10}^e h_{10}^e \rangle \langle h_{10}^i h_{10}^i \rangle \\ \langle h_{10}^i h_{10}^e \rangle \langle h_{10}^e h_{10}^i \rangle \end{pmatrix}^{-1} \begin{pmatrix} \langle h_{10}^e h_{21}^e \rangle \langle h_{10}^i h_{21}^i \rangle \\ \langle h_{10}^i h_{21}^e \rangle \langle h_{10}^e h_{21}^i \rangle \end{pmatrix}$, with brackets denoting integrals over the colatitude range of data used ($25^\circ - 155^\circ$).

[15] For perfectly coherent long period variations of q_{10} and q_{21} with amplitude ratio $1:\beta$, the expectation of the internal/external TFs estimate at magnetospheric longitude ϕ is found to be

$$\hat{Q}_1 = (Q_1 + c_2(\phi)\beta)/(1 + c_1(\phi)\beta). \quad (8)$$

Rough estimates of the LT dependence of the frequency independent proportionality constants plotted in Figure 1 are also readily derived

$$\alpha_e(\phi) \approx (1 + \beta c_1(\phi))/(1 + |Q_1|) \quad (9)$$

$$\alpha_i(\phi) \approx (|Q_1| + \beta c_2(\phi))/(1 + |Q_1|) \quad (10)$$

where Q_1 is the internal/external transfer function for a representative period for D_{st} variations, roughly 5–10 days. Equations (8)–(10) depend on the induction TF Q_1 and $Q_2(\omega_r)$, and two unknown parameters: β (the relative amplitude of the quadrupole component), and ϕ_0 (the quadrupole orientation). The theory is easily extended to allow for the more general case where the coherence ρ between q_{10} and q_{21} is less than one (or frequency dependent, and complex). Q_1 and Q_2 are easily computed for a standard mantle conductivity profile or directly from data; our results are insensitive to the choice within reasonable bounds. To roughly estimate β and ϕ_0 , we plot the predicted $\alpha_e(\phi)$ for various values of the unknowns and compare to estimates from CHAMP (i.e., Figure 1). Values of $\phi_0 = -67.5^\circ$ (corresponding to a peak in the quadrupole

amplitude at 19:30 LT) and $\beta = 0.125$ provide the best fit to the external CHAMP D_{st} proportionality constants, and also reproduce the weak LT dependence of the internal ratio $\alpha_i(\phi)$.

[16] The predicted LT dependence of low frequency ($\ll 1$ cpd) estimates of Q_1 are then easily computed using equation (8) and converted into the C_1 -responses. Results for the 3 LT bands for which C_1 estimates were obtained from CHAMP are presented as symbols in Figure 2, for several representative periods. Our simple theory at least qualitatively explains the observed variation of long period C-response functions with LT. A significantly better fit is obtained for slightly modified values of model parameters ($\beta = 0.1$ and $\phi_0 = -60^\circ$; Figure 2). The only significant anomaly is in the imaginary part of the C-response for LT band 4:00–8:00, which probably can be attributed to the low signal strength in this LT sector. Note that there are also significant LT variations at frequencies above 1 cpd. Undoubtedly higher order spatial structure is at least as important at these higher frequencies, but accounting for rotational effects on the inductive response would be somewhat more complicated for this case.

5. Discussion

[17] Our results provide evidence for a significant non-axisymmetric quadrupole component in long period magnetic field variations, and demonstrate that these can lead to LT dependent biases in satellite induction TF estimates. Two lines of evidence support the conclusion that the currents giving rise to this quadrupole component are in the magnetosphere, as we have assumed here. First, equation (5) can be modified, so that both the inducing and induced quadrupole terms are interior to the satellite orbit, as would be the case for an ionospheric source. This modification results in changes to the expressions for $c_1(\phi)$ and $c_2(\phi)$ in (6)–(10) such that the very weak dependence of α_i on LT cannot be reproduced for any choice of model parameters. Second, the strong dependence of α_e on LT requires coherence of the non-axisymmetric sources with D_{st} , while modulations in ionospheric daily variation fields are only weakly correlated with this index [Daglis and Kozyra, 2002].

[18] We estimate that the amplitude of the coherent quadrupole component is about 10–15% of the dipole (for the Schmidt normalization used here). Since coherence with the symmetric ring current component is unlikely to be perfect, actual quadrupole source variations are probably of greater amplitude, and may well also contain some contributions from ionospheric sources. In the context of our analysis, these additional incoherent sources appear as noise, rather than bias.

[19] Whether vector or scalar data are used for satellite induction studies, the source model should obviously be extended to allow for non-axisymmetric sources, introducing at least a Y_2^1 quadrupole component. However, including these additional terms raises a number of additional issues. For example, we have ignored the distinction between the Earth's rotation and geomagnetic dipole axes in our derivations. Also, as we have noted above, non-axisymmetric fields may result from both magnetospheric and ionospheric sources. Separating these will be essential to making full use of satellite data in induction studies. For example, non-axisymmetric structure in low frequency magnetospheric fields will appear in an Earth fixed frame as harmonics of

1 cpd. These magnetospheric sources may thus be included to some extent in daily variation corrections, with external components erroneously assumed to be below the ionosphere as part of the S_q current system. Clearly this possibility has significant implications for satellite induction studies at daily variation periods that are presently being pursued [Everett *et al.*, 2003].

[20] A better understanding of magnetospheric and ionospheric sources will be required before magnetic satellite induction studies reach their full potential. As our results demonstrate, interpretation of data under erroneous source assumptions can lead to substantial biases. Geodynamically significant variations in mantle conductivity will result in relatively subtle changes in induction TFs, so even small biases have the potential to be very misleading. As satellite induction studies become more ambitious and three dimensional Earth models are considered this issue will become even more important.

[21] **Acknowledgments.** This research was supported by DFG's research grant MA 2117/3, as part of the Priority Program SPP 1097 and a visiting professorship at GFZ Potsdam for G.E. Helpful discussions with J. Schwarte and H. Lühr and comments from two anonymous reviewers are gratefully acknowledged.

References

- Balasis, G., S. Maus, H. Lühr, and M. Rother (2004), Wavelet analysis of CHAMP flux gate magnetometer data, in *Earth Observation with CHAMP*, edited by C. Reigber, H. Lühr, P. Schwintzer and J. Wickert, pp. 347–352, Springer, New York.
- Banks, R. J. (1969), Geomagnetic variations and the conductivity of the upper mantle, *Geophys. J. R. Astron. Soc.*, *17*, 457–487.
- Campbell, W. H. (1997), *Introduction to Geomagnetic Fields*, 304 pp., Cambridge Univ. Press, New York.
- Constable, S., and C. Constable (2004), Observing geomagnetic induction in magnetic satellite measurements and associated implications for mantle conductivity, *Geochem. Geophys. Geosyst.*, *5*, Q01006, doi:10.1029/2003GC000634.
- Daglis, I. A., and J. U. Kozyra (2002), Outstanding issues of ring current dynamics, *J. Atmos. Sol. Terr. Phys.*, *64*, 253–264.
- Egbert, G. D. (1997), Robust multiple-station magnetotelluric data processing, *Geophys. J. Int.*, *130*, 475–496.
- Everett, M., S. Constable, and C. Constable (2003), Effects of near-surface conductance on global satellite induction responses, *Geophys. J. Int.*, *153*, 277–286.
- Fujii, I., and A. Schultz (2002), The 3D electromagnetic response of the Earth to ring current and auroral oval excitation, *Geophys. J. Int.*, *151*, 689–709.
- Langel, R. A., and W. J. Hinze (1998), *The Magnetic Field of the Earth's Lithosphere: The Satellite Perspective*, 429 pp., Cambridge Univ. Press, New York.
- Maus, S., and P. Weidelt (2004), Separating the magnetospheric disturbance magnetic field into external and transient internal contributions using a 1D conductivity model of the Earth, *Geophys. Res. Lett.*, *31*, L12614, doi:10.1029/2004GL020232.
- Olsen, N. (1998), The electrical conductivity of the mantle beneath Europe derived from C-responses from 3 to 720 hr, *Geophys. J. Int.*, *133*, 298–308.
- Olsen, N. (1999), Induction studies with satellite data, *Surv. Geophys.*, *20*, 309–340.
- Schwarte, J. (2004), Modeling the Earth's magnetic field of magnetospheric origin from CHAMP data, Ph.D. thesis, 130 pp., Tech. Univ. of Braunschweig, Germany.
- Tsyganenko, N. A. (2002), A model of the near magnetosphere with a dawn-dusk asymmetry: 2. Parameterization and fitting to observations, *J. Geophys. Res.*, *107*(A8), 1176, doi:10.1029/2001JA000220.

G. Balasis, GeoForschungsZentrum Potsdam, Telegrafenberg, D-14473 Potsdam, Germany. (gbalasis@gfz-potsdam.de)

G. D. Egbert, College of Oceanic and Atmospheric Sciences, Oregon State University, Oceanography Administration Building 104, Corvallis, OR 97331-5503, USA.

S. Maus, National Geophysical Data Center, NOAA E/GC1, 325 Broadway, Boulder, CO 80305-3328, USA.